Millimetre and submillimetre molecular line observations of the reflection nebula NGC 2023

Astron. Astrophys. 227, 200–206 (1990)

ASTRONOMY AND ASTROPHYSICS

Millimetre and submillimetre molecular line observations of the reflection nebula NGC 2023

Glenn J. White [1], Carl Sanderson [1,*], T.S. Monteiro [2], K.J. Richardson [1], and S.S. Hayashi [3]

[1] Molecular Astronomy Group, Department of Physics, Queen Mary and Westfield College, University of London, Mile End Road, London, E1 4NS, England, UK
[2] Department of Mathematics, Royal Holloway and Bedford New College, Egham, Surrey TW20 0EX, England, UK
[3] James Clerk Maxwell Telescope Unit, 665, Komohana Street, Hilo, Hawaii, USA

Received May 11, accepted July 3, 1989

Abstract. Observations in the CO $J=2-1$, CO $J=3-2$ and HCO^+ $J=4-3$ transitions of the molecular cloud associated with NGC 2023 are presented. The observations reveal the complex structure of the gas in the surrounding cloud, and show the presence of several hot-spots which may represent separate bodies of gas. A search has been made for the source of excitation of two nearby groups of Herbig-Haro objects recently discovered by Malin et al. (1987). No such object can be clearly identified from our data. CO $J=3-2$ spectra taken at positions lying on the CO $J=1-0$ shell observed by Gatley et al. (1987) show marked enhancements in peak line strength relative to coincident CO $J=2-1$ data. By contrast, no such enhancements are observed away from the shell. Observations of the submillimetre wavelength HCO^+ $J=4-3$ transition show that the line strength is greatest in the vicinity of the shell structure. Simple LVG modelling of the excitation conditions of the shell material suggests that the gas may be hot ($T_{kin} \sim 140$ K), dense and optically thin.

Key words: interstellar medium – molecules – radio lines: molecular – nebulae: reflection

1. Introduction

The reflection nebula NGC 2023 was first studied by Hubble (1922), and since then has been the subject of considerable interest. Morris et al. (1975) mapped the structure of the nearby dense molecular cloud, and photometric studies by Lee (1968) revealed the presence of anomalously high ultra-violet extinction. Emerson et al. (1975) carried out a 40–350 μm photometric study of NGC 2023, which revealed a prominent infra-red excess. Comparing the energy absorbed in the ultra-violet to the total integrated energy in the infra-red excess, and finding that the were roughly equal, Emerson et al. concluded that this excess resulted from emission by dust grains. Observations by Knapp et al. (1975) revealed a C II region lying outside a H II region, and Milman et al. (1975) showed that a peak in CO $J=1-0$ emission occurred at a point lying 1′ south of the B1.5 star HD 37903, believed to be the ionising star. A core-halo model for the C II region was proposed by Pankonin and Walmsley (1976, 1978), based on the evidence of double-peaked carbon recombination lines. Harvey et al. (1980) first applied the so-called "blister" model of star formation to this source, and White et al. (1980, 1981) performed the first multi-transition CO studies. Gatley et al. (1987) detected vibrationally-excited molecular hydrogen lying in a narrow ridge adjacent to a shell of CO gas. They concluded that UV fluorescence is responsible for the excitation of the H_2.

The model that has emerged from this work is as follows. The CO gas in the shell is being compressed and excited by some mechanism yet to be determined, such as, for example, the expansion of ionised material initiated by radiation pressure from the central star. At the same time, two effects due to the action of UV photons emanating from HD 37903 may be important. Photon absorption and re-emission by the dust inside the H II region probably generates the IR excess observed by Emerson et al. (1975); and UV radiation from the star may also be responsible for the excitation of the molecular hydrogen, producing the observed fluorescent H_2 spectra and resultant spatial distribution of neutral gas observed by Gatley et al. (1987). Pre-existing condensations in the parent molecular cloud may result in density variations across the ionisation front, causing the shell to have a broken, irregular appearance.

The observational features of the source expected on the basis of this model include an infrared excess, a shell or ring of molecular gas, and fluorescent H_2 emission interposed between this shocked gas and HD 37903. It would clearly be useful to study this source in lines of easily excited, low dipole moment molecules, such as CO. By observing this region in different rotational transitions of CO, it may be possible to infer the physical conditions in the source, search for any evidence of the presence of hot, shocked gas, and to constrain the excitation conditions in the emitting gas. Such observations may provide a useful test of the model described earlier.

2. Observations

The CO $J=2-1$ observations presented in this paper were obtained in 1985 May using the 12 m telescope of the National Radio Astronomy Observatory (NRAO), at Kitt Peak, Arizona. The receiver was dual-channel cryogenic Schottky-diode system having a noise temperature of about 1000 K. The velocity resolution used was 0.325 km s^{-1} with a typical integration time for each spectrum of 3 min. The forward scattering and spillover efficiency η_{fss} of the telescope (Kutner and Ulich, 1981) was 0.73

Send offprint requests to: G.J. White

* Present address: Department of Mathematics, UMIST, P.O. Box 88, Manchester M60 1QD, UK

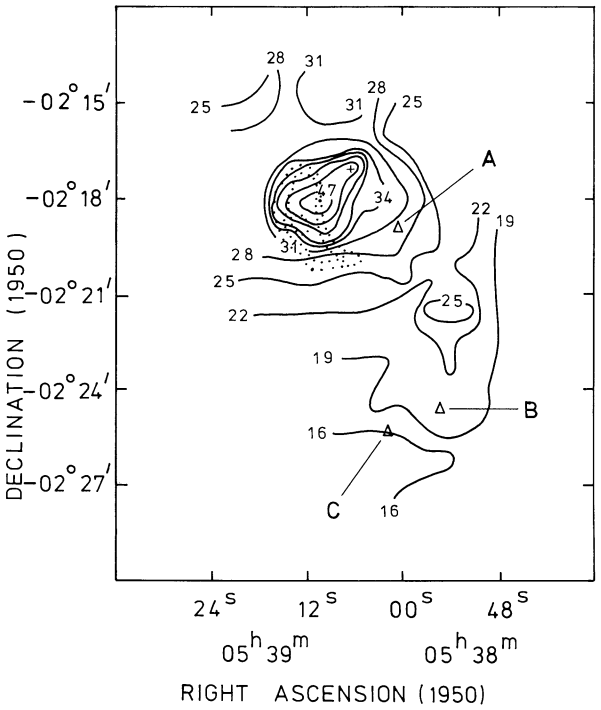

Fig. 1. A map of peak T_R^* (CO $J=2-1$) covering the NGC 2023 region. The dotted lines show the approximate extent of the CO $J=1-0$ shell reported by Gatley et al. (1987). A, B and C denote groups of H-H objects (see text). The plus (+) sign indicates the position of HD 37903

at this frquency. With this system, the telescope half-power beamwidth was 30″, and the pointing was determined to be good to about $\frac{1}{4}$ of the beamwidth. Over 125 positions were observed, sampling every 1′ except in those regions of the source which showed complex contour structure, where 30″ spacing was used. To facilitate comparison with the $J=2-1$ data, CO $J=3-2$ spectra were obtained during 1985 October using the United Kingdom Infra-Red Telescope (UKIRT), situated on Mauna Kea, Hawaii, with the Queen Mary College Submillimetre Spectral Line Receiver (White et al., 1986). For these observations, the HPBW was 53″, and η_{fss} was estimated to be 0.88. In order to compare spectra from the two lines it was necessary to convolve together a number of the CO $J=2-1$ spectra to synthesise the larger beamsize of the CO $J=3-2$ observations. This convolution was carried out for eight separate positions at which CO $J=3-2$ spectra had been obtained. All results presented in this paper are given in units of T_R^* (Kutner and Ulich, 1981).

3. Results

3.1. Distribution of peak line intensity

A map of peak T_R^* (CO $J=2-1$) has been made, covering an area of 9′ × 13′ (RA × Dec) (see Fig. 1). The dominant feature of this map is the region of bright emission showing complex contour structure close to the position of the reflection nebula NGC 2023. The CO $J=1-0$ emission observed by Gatley et al. (1987) is also illustrated schematically. In this region the observed line intensities imply that the gas kinetic temperature may be at least 50 K, making the source relatively hot-centred. The observational characteristics of this region will be described in greater detail in later sections. The CO emission is brightest around the reflection nebula, concentrated into a region having a diameter of about 6′, corresponding to 0.8 pc. Outside this region, the line intensities suggest that the gas kinetic temperature decreases to 15–25 K. Two other CO hot-spots are apparent, one being a bar-like feature running in a N-S direction, centred about 7′ SW of NGC 2023.

This region covers the positions of a group of Herbig-Haro objects discovered by Malin et al. (1987), which are discussed in more detail in a later section. The other intensity peak lies to the north of the cloud, and may be associated with the edge of the extended molecular complex NGC 2024, which will be discussed in a separate paper (White et al., 1989).

3.2. Channel maps

Figure 2 shows channel maps of NGC 2023 with velocity resolution 0.65 km s^{-1}. An extended CO hot-spot is observed at the approximate position of the reflection nebula. Comparison between our 9.8 km s^{-1} map and a CO $J=1-0$ map of the source (Gatley et al., 1987) reveals similarities in the spatial distribution of emission from the two transitions. In our channel map there is an emission peak at the position of the CO $J=1-0$ shell. The morphology of the CO $J=2-1$ contours suggests that we may be seeing the same shell structure in the higher transition, but in view of our lower spatial resolution, this evidence is not entirely conclusive. We believe, however, that we see signs of emission from the shell-source, and that high angular resolution CO $J=2-1$ studies of this region will establish its presence in this transition beyond doubt. CO $J=2-1$ emission associated with this "shell" shows up most clearly in our 10.5 and 9.8 km s^{-1} channel maps, although enhanced emission from its vicinity can be seen in the velocity range 5.7–10.5 km s^{-1}. However, the position of peak T_R^* (CO $J=2-1$) close to the shell-source changes non-systematically with *lsr* velocity. This effect evokes the presence of a number of different clumps of emitting gas with different *lsr* velocities. Although the scenario described in Sect. 1 is favoured by our evidence, the source structure is clearly more complex than this simplistic model implies.

An extended ridge of CO emission, present on several channel maps, runs roughly NW-SE across the centre of the region. It is clearly apparent in the 6.5 km s^{-1} channel, and appears prominently in several others. The ridge-like feature ends close to a bright hot-spot lying at the position RA (1950) $05^h38^m55^s$, Dec (1950) −02°20′ which can be clearly seen over the range 4.6–7.2 km s^{-1}. The value of T_R^* (CO), which is typically up to 10 K, varies rapidly with *lsr* velocity in this region. This feature lies about 1.5′ north of the hot-spot seen in Fig. 1 at RA (1950) $05^h38^m53^s$, Dec (1950) −02°21′30″, where $T_R^* \sim 25$ K. The positional variation of the hot-spots indicates the presence of several separate kinematical components, suggesting that fragmentation and clumping are widespread.

3.3. Relationship to Herbig-Haro objects

Malin et al. (1987) measured the proper motions of two groups of Herbig-Haro (H-H) objects which they had discovered in the vicinity of NGC 2023. The more northerly group, designated A (see Fig. 1), show proper motions which indicate movement away from the central ionised regions of NGC 2023. It is thus reasonable to conclude that the H-H objects may have been accelerated outwards from this centre of activity. The H-H complex situated about 8′.5 SW of NGC 2023 contains two separate groups of objects (B and C), whose proper motions suggest that they are

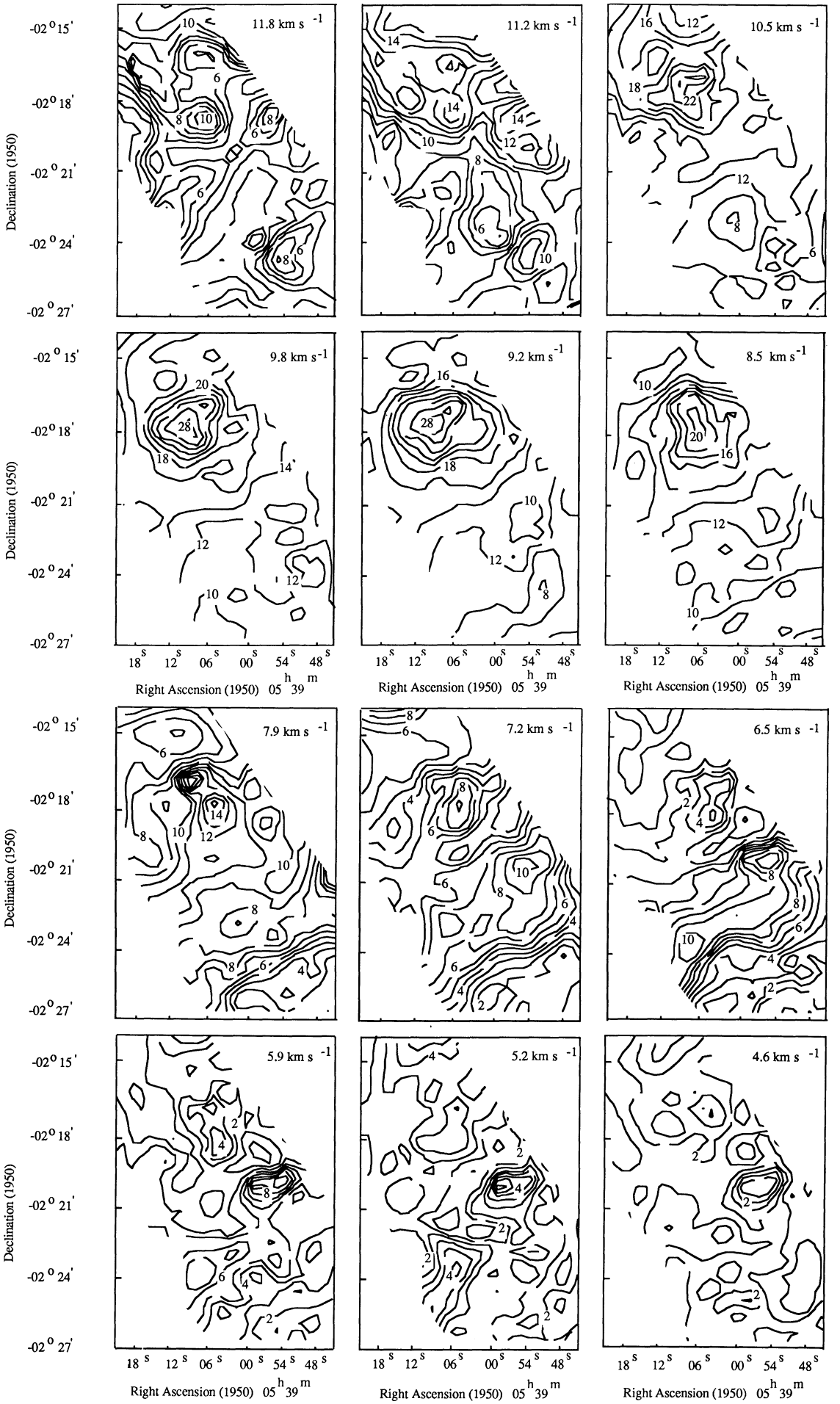

Fig. 2. Channels maps of the CO $J=2-1$ transition in NGC 2023, integrated into velocity intervals 0.65 km s^{-1} wide

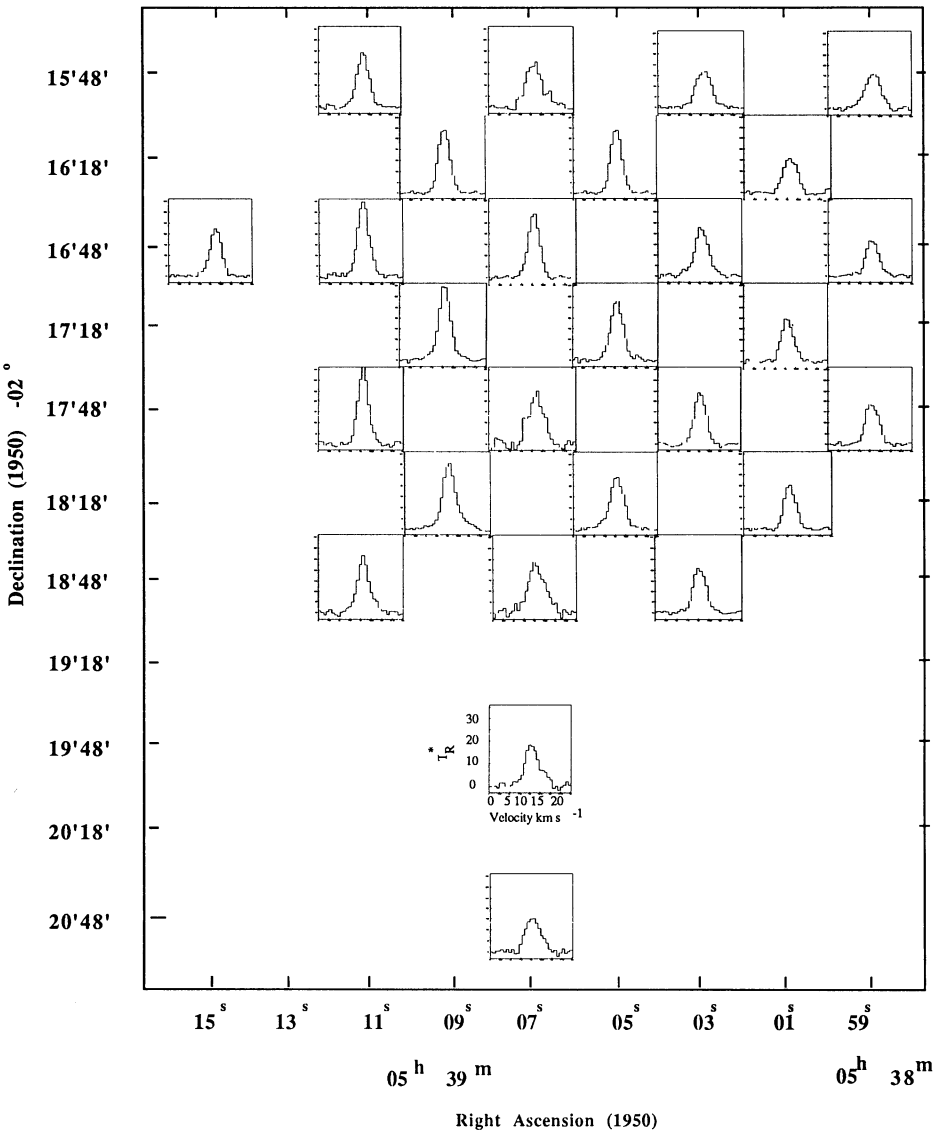

Fig. 3. CO $J=3-2$ spectra observed toward NGC 2023 using UKIRT. The linestrength of this transition peaks up in the vicinity of the CO $J=1-0$ shell

moving in mutally opposite directions, ruling out the possibility that NGC 2023 is responsible for their acceleration. It is possible that an as yet undetected source driving the H-H objects is situated between them.

Our CO $J=2-1$ maps have been examined for evidence attributable to such a central exciting source. However, the channel maps do not show any obvious intense CO peak positioned between the two groups of H-H objects. Higher-angular resolution observations of this region may help to identify such a CO hot-spot. Optical photographs of this area show several patches of bright nebulosity lying close to V615 Ori, a variable star situated about 0.13 pc from the H-H objects, which may be associated with the nebulosity.

3.4. CO $J=3-2$ observations

UKIRT observations of the CO $J=3-2$ transition have been made towards selected positions in NGC 2023 (Fig. 3). The highest line temperatures are observed toward the position of the shell-source. In order to compare these data with the CO $J=2-1$ spectra, it was necessary to convolve the latter to the same spatial resolution as the CO $J=3-2$ observations. The results of this profile synthesis are shown in Fig. 4. The four pairs of spectra shown at the top were obtained at positions at the inside edge of the CO $J=1-0$ shell, and those on the bottom were taken at randomly selected positions about 0.1 pc west of the shell, in the more ambient gas. Those spectra observed towards the "shell" show a clear excess in the ratio $R_{32}=\dfrac{T_R^*(\mathrm{CO}\,J=3-2)}{T_R^*(\mathrm{CO}\,J=2-1)}$, which reaches almost 1.9 at the position 60E60N. By contrast, the ambient parts of the cloud displaced by $\sim 2'$ from the shell exhibit no such enhancement. We stress the *systematic* difference between the relative intensities of the $J=3-2$ and $J=2-1$ spectra observed towards the shell, and those observed in nearby ambient cloud material.

3.5. HCO^+ $J=4-3$ observations

Figure 5 shows HCO^+ $J=4-3$ spectra obtained as part of a north-south strip running from 120N to 240S (relative to the origin of the CO $J=3-2$ observations). The HCO^+ $J=4-3$ transition was detected toward several positions, with T_R^* in the

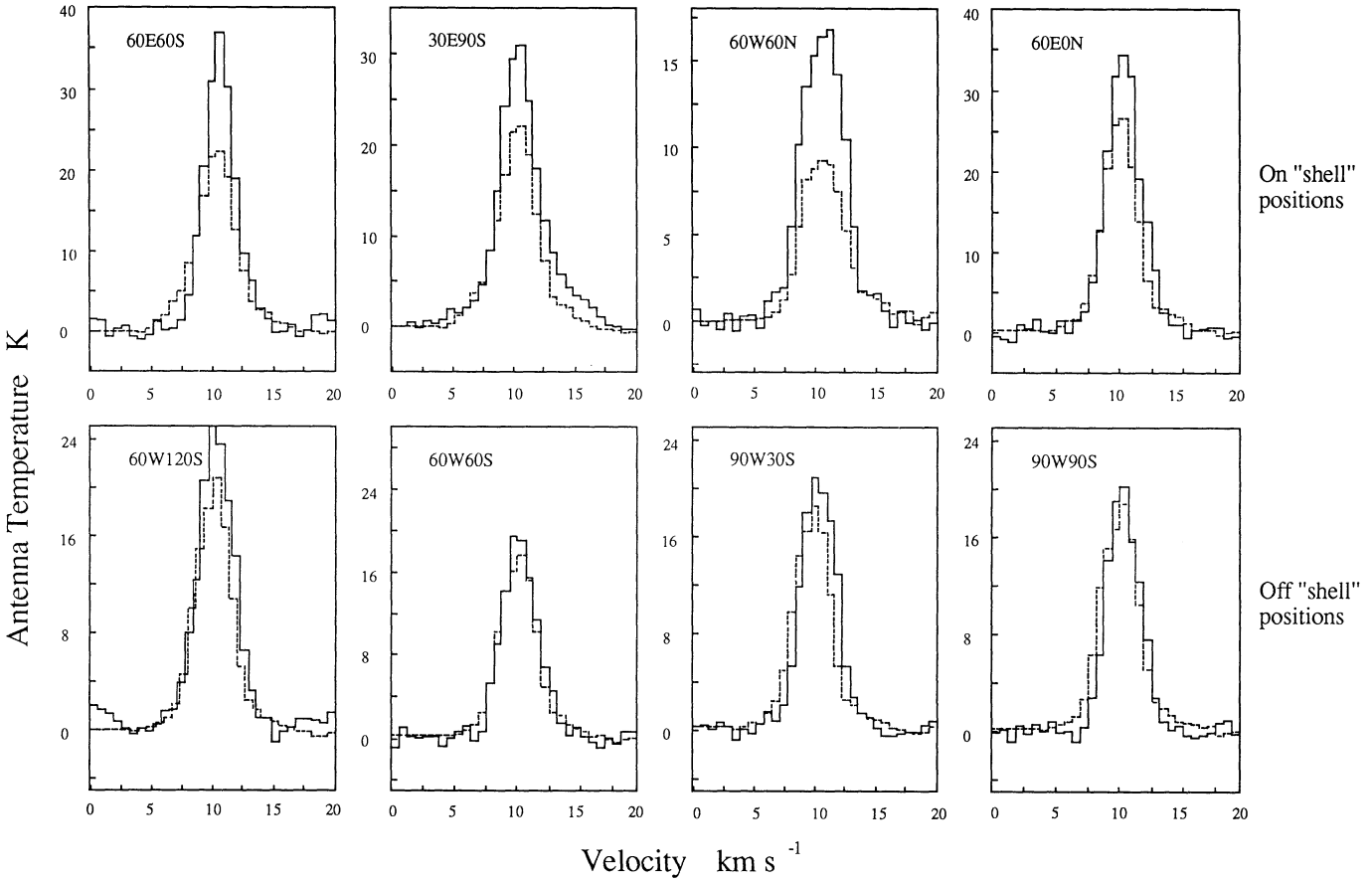

Fig. 4. Montages of CO $J=3-2$ and $J=2-1$ spectra observed toward selected positions in NGC 2023. The CO $J=2-1$ spectra have been convolved together to match the larger beamsize of the UKIRT observations (see text). The CO $J=3-2$ lines show a marked enhancement relative to the CO $J=2-1$ spectra on the shell-source

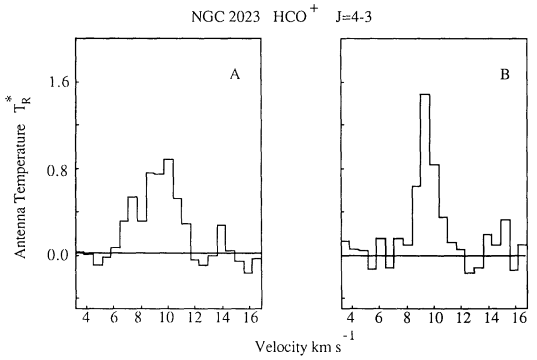

Fig. 5. HCO^+ $J=4-3$ spectra observed towards selected positions, 60S (A) and 120S (B) in NGC 2023. The excitation of HCO^+ varies rapidly close to the CO $J=1-0$ shell-source

range 0.9–1.5 K. The emission is strongest at positions 60S (A) and 120S (B). The linewidths for these spectra (FWHM = 3.0 and 1.2 km s^{-1} respectively) are markedly different, demonstrating that the excitation may vary rapidly close to the shell-source.

3.6. IRAS observations

Figure 6 shows IRAS maps of the thermal emission from NGC 2023, at 12, 25, 60 and 100 μm (Fig. 6). The raw satellite data

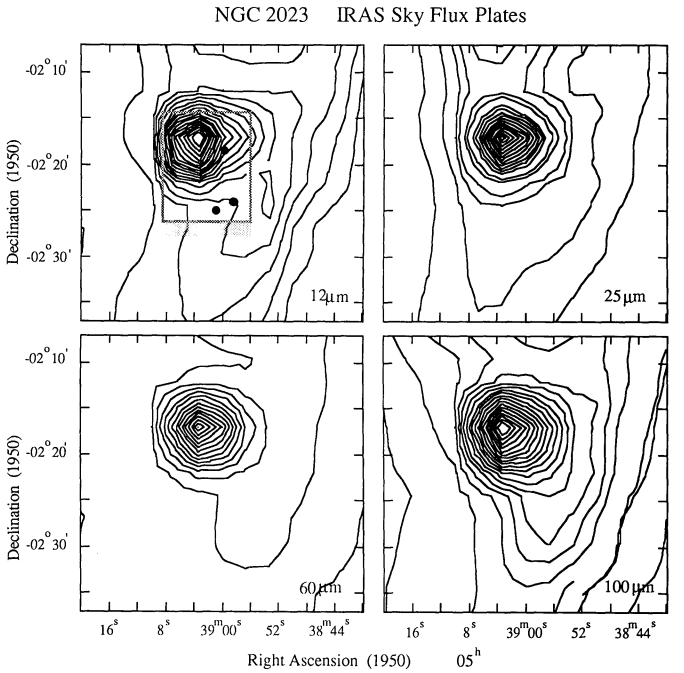

Fig. 6. IRAS maps of NGC 2023. See text for peak surface brightnesses

were processed using the CRDD reduction procedure (Starlink User Note 91.1), which produces higher angular resolution images than the Sky Flux Plates. The effective resolution achieved by this technique varies from a $1' \times 4'$ elliptical beam (with the larger axis aligned E-W) at 12 μm to a 5′ circular beam at 100 μm.

The dominant feature of the dust emission is the intense peak observed in all four wavebands at the position of NGC 2023, about 3′ east of HD 37903. The peak surface brightness in the four wavebands is 160, 335, 1617, and 1863 MJy sr^{-1} in the 12, 25, 60, and 100 μm bands respectively. These maps were examined for signs of the bar observed in the SW region of Fig. 1, extending southwards towards the H-H objects, but no such bar is apparent. A fit for IR colour temperature carried out by Mozurkewich et al. (1986) agrees with our value for the brightness temperature of ~50 K obtained from the molecular line observations, within the very considerable errors associated with the IRAS data.

We note, however, that the FIR maps do show evidence for a prominent bar extending southwards, and displaced by about 10′ to the southwest of NGC 2023. This bar lies outside the area covered by the molecular line observations (Fig. 1).

4. Discussion

The immediate impression gained from an examination of the contour maps is one of complexity and irregularity. Several interesting features are observed, such as the emission associated with the CO $J=1-0$ shell-source dicovered by Gatley et al. (1987); the ridge of bright emission; and the compact, localised hot-spots apparent at several positions. However, the detailed structure is often a very complex function of *lsr* velocity; it is therefore very difficult to apply any unique model to the data, and we are restricted to rather more global conclusions. Our maps covering the region where Gatley et al. (1987) detected the CO $J=1-0$ shell and UV fluorescence certainly show complex CO $J=2-1$ and $J=3-2$ spatial structure. At 10.5 km s^{-1} there is a suggestion of the CO shell, although higher angular resolution than that of the CO $J=2-1$ observations is required to confirm this unequivocally. This might represent supportive evidence for the model described earlier. However, the precise scenario for this source remains far from clear. It is likely that fragmentation is giving rise to widespread, large-scale clumping. This can account for the broken and irregular appearance of the CO shell-source, as well as the observed velocity structure.

The high values of R_{32} observed close to the main centre of activity may be interpreted as a further indication of hot gas. The enhanced strength of the higher transition is indicative of higher excitation temperatures in this region (if the gas is optically thin). To test this conclusion, a simple Large Velocity Gradient (LVG) analysis (Goldreich and Kwan, 1974; Richardson, 1985) was carried out. For different values of the kinetic temperature, the radiation temperature T_R, optical depth τ and excitation temperature T_{ex} were calculated as functions of the hydrogen density n_{H_2} and the relative CO abundance per unit velocity gradient $X(\mathrm{CO})\Big/\frac{dv}{dr}$. The results of this analyis are shown in Fig. 7. Adopting the values $X(\mathrm{CO}) = 2\ 10^{-5}$ (Gerola and Glassgold, 1978) and $\frac{dv}{dr} = 30\ \mathrm{km\,s^{-1}\,pc^{-1}}$, based on the observed linewidths and size of the emitting region, we found that the observed line ratios could not be reproduced with the model using an assumed kinetic temperature of less than 140 K, consistent with hydrogen densities of 10^4–10^5 cm^{-3}. This estimate is, of course, subject to

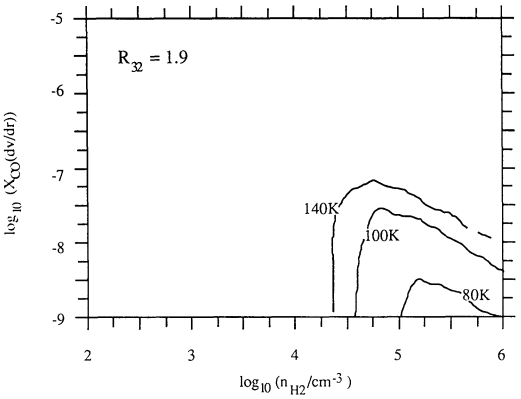

Fig. 7. A Large Velocity Gradient analysis of the CO spectra observed toward NGC 2023. The simple LVG model cannot reproduce the observed line ratios for an assumed kinetic temperature of less than 140 K

the considerable uncertainties associated with LVG techniques, perhaps half an order of magnitude in $X(\mathrm{CO})\Big/\frac{dv}{dr}$. The modelling also showed that both CO transitions are fairly optically thin ($\tau \sim 0.5$), so the line intensity should increase with kinetic temperature. The lower limit on the kinetic temperature is, however, much higher than the observed line intensities on the "shell". The latter presumably result from a combination of incomplete thermalisation and dilution in the 53″ beam, which is likely to be severe, given the obviously clumpy nature of the emitting gas. The emitting region may be quite narrow (Gatley et al., 1987), thereby exacerbating beam dilution effects. The similarity between the CO $J=3-2$ and convolved $J=2-1$ line profiles at positions away from the shell (Fig. 4) suggests that the emission from the two transitions is broadly co-spatial. If this is the case in the shell, then the high values of R_{32} probably represent a true enhancement, and not merely a consequence of a less optically thick CO $J=3-2$ line sampling hotter material in the cloud. It is true that LVG techniques are inherently unrealistic for modelling molecular lines (especially optically thick transitions) because of the assumptions of uniform density, temperature and velocity fields, which ignore local radiative transfer effects. In reality, of course, sources will have complex density and temperature structure; the present source is a case in point. Nevertheless, it is thought that LVG techniques provide a useful first estimate of the physical conditions prevailing in gaseous nebulae such as NGC 2023. We therefore interpret the observed line ratios as being due to hot, optically thin gas which may have been shocked. The results of the modelling are consistent with a scenario in which the CO gas is compressed and heated. One possible mechanism is the expansion of ionised material initiated by stellar radiation pressure. A more sophisticated model, taking account of fragmentation, clumping, turbulence, radiative heating, CO shielding and dust processing might provide a more realistic picture.

We have attempted to estimate the physical size of the emitting zone for this highly-excited gas, using the LVG analysis to predict the radiation temperature T_R, and comparing this with the observed spectra. In order to model this it was assumed that the highly excited gas is in the form of a narrow shell which sits across the beam, and is surrounded by ambient cloud material having a kinetic temperature of 35 K, a value based on the intensity of spectra taken immediately adjacent to the shell. Using this model, an upper limit of 10″ (0.02 pc) can be set for the width of such a narrow shell. However, this technique is strongly dependent on

the kinetic temperature of any surrounding material present in the beam, and must be regarded for the time being as uncertain. Clearly, however, high-resolution observations would be an advantage in determining the extent of the emitting region.

Further supportive evidence in favour of high excitation close to the shell is provided by the HCO^+ $J=4-3$ spectra. The three positions which show the highest line strengths lie on the inside edge of the shell-like structure that was observed in the CO $J=2-1$ transition. A simple LVG analysis of these data for an assumed kinetic temperature of 30 K, suggests that n_{H_2} is about 6–8 $10^4\,cm^{-3}$, assuming the HCO^+ abundance to be $6\,10^{-9}$ (Wootten et al., 1984; Loren et al., 1984).

5. Conclusions

There are clear similarities between the CO $J=2-1$ contours maps presented in this paper and the CO $J=1-0$ map by Gatley et al. (1987). The presence of a shell-like structure is consistent with the observations of both lines, though less clearly in the higher transition. The data are consistent with a model in which the molecular material is being compressed and excited by some mechanism, such as stellar radiation pressure.

The multiplicity of CO hot-spots and their positional variation are indicative of widespread fragmentation and large-scale clumping. This introduces additional complexity into any modelling. However, the evidence still favours this shocked blister model, further support for which is provided by the high line ratios generated in the shell-structure. The LVG model and observations point towards the presence of hot, dense, optically thin gas which may have undergone a shock impact.

The intensity peak lying SW of the reflection nebula, also has complex spatial and velocity structure, which can be understood in terms of fragmentation and clumping. It appears to be unassociated with the reflection nebula NGC 2023.

The evidence may be consistent with a shock model for this source, although it is possible that the observed emission line ratios may arise from ultraviolet-induced photodissociation in the dense molecular cloud (Hartquist, 1988). It is clear that studies of this region are far from complete, and that much work remains to be done before a reliable model for NGC 2023 can be formulated, taking account of the unmistakable evidence for the action of fragmentation and clumping.

Acknowledgements. We thank the SERC for financial support for millimetre and sub-millimetre wavelength astronomy at QMC, and for a research studentship for CAS; the NRAO for allocation and support of observing time at Kitt Peak; J. Walsh for discussions on the NGC 2023 region; the UKIRT Unit for support and assistance; P. Richards at RAL for help with the IRAS data reduction; and L. Avery for help at the Kitt Peak 12m telescope. CAS wishes to thank VBS for many helpful discussions. We acknowledge useful comments from the referee which have improved the discussion of the data.

References

Emerson, J.P., Furniss, I., Jennings, R.E.: 1975, *Monthly Notices Roy. Astron. Soc.* **172**, 411
Gatley, I., Hasegawa, T., Suzuki, H., Garden, R., Brand, P.W.J.L., Glencross, W., Okuda, H., Nagata, T.: 1987, *Astrophys. J.* **317**, L73
Gerola, H., Glassgold, A.E.: 1978, *Astrophys. J. Suppl.* **37**, 1
Goldreich, P., Kwan, J.: 1974, *Astrophys. J.* **189**, 441
Hartquist, T.W.: 1988, in *Millimetre and Submillimetre Astronomy, Proceedings of Stirling Summer School*, eds. R. Wolstencroft, W. Burton. Reidel, Dordrecht
Harvey, P.M., Thronson, H.A., Gatley, I.: 1980, *Astrophys. J.* **235**, 894
Hubble, E.: 1922, *Astrophys. J.* **56**, 162
Knapp, G.R., Brown, R.L., Kuiper, T.B.H.: 1975, *Astrophys. J.* **196**, 167
Kutner, M.L., Ulich, B.L.: 1981, *Astrophys. J.* **250**, 341
Lee, T.A.: 1968, *Astrophys. J.* **152**, 913
Loren, R.B., Wootten, H.A., Sandqvist, Aa., Friberg, P., Hjalmarson, A.: 1984, *Astrophys. J.* **287**, 707
Malin, D.F., Ogura, K., Walsh, J.R.: 1987, *Monthly Notices Roy. Astron. Soc.* **227**, 361
Milman, A.S., Knapp, G.R., Kerr, F.J., Knapp, S.L., Wilson, W.J.: 1975, *Astron. J.* **80**, 93
Morris, M., Palmer, P., Turner, B.E., Zuckerman, B.: 1975, *Astrophys. J.* **191**, 349
Mozurkewich, D., Schwartz, P.R., Smith, H.A.: 1986, *Astrophys. J.* **311**, 371
Pankonin, V., Walmsley, C.M.: 1976, *Astron. Astrophys.* **48**, 341
Pankonin, V., Walmsley, C.M.: 1978, *Astron. Astrophys.* **67**, 129
Richardson, K.J.: 1985, Ph.D. Thesis, Queen Mary College, University of London
White, G.J., Watt, G.D., Beckman, J.E., Rose, B., van Vliet, A.: 1980, *Astron. Astrophys.* **84**, 212
White, G.J., Phillips, J.P., Watt, G.D.: 1981, *Monthly Notices Roy. Astron. Soc.* **197**, 745
White, G.J., Monteiro, T.S., Richardson, K.R., Griffin, M.J., Rainey, R.: 1986, *Astron. Astrophys.* **162**, 253
White, G.J., Sanderson, C.A., Hayashi, S.S., Richardson, K.J., Monteiro, T.S.: 1989, *Astron. Astrophys.* (submitted)
Wootten, H.A., Loren, R.B., Sandqvist, Aa., Friberg, P., Hjalmarson, A.: 1984, *Astrophys. J.* **279**, 633